Fraying and Electron Autodetachment Dynamics of Trapped Gas Phase Oligonucleotides

Allison S. Danell and Joel H. Parks
Rowland Institute at Harvard, Cambridige, Massachusetts, USA

Sensitive methods recently developed to measure laser-induced fluorescence from trapped ions have been applied to study the dynamics of double- and single-stranded oligonucleotides. In this paper, the fraying of duplex terminal base pairs has been identified by measuring the donor fluorescence as a function of temperature from an oligonucleotide duplex labeled with a pair of FRET dyes. Comparison of the degree of dissociation of 14-mer duplexes observed in the mass spectra with the fluorescence intensity of the donor enables intermediate conformations of the unzipping duplex at the weaker binding end of the duplex to be identified. The autodetachment of electrons from double- and single-stranded oligonucleotide anions has been observed in a gas phase environment. To characterize this process, measurements were performed on 7-mers prepared without FRET fluorophores attached. The dependence of the decay rates of trapped anions have been measured as a function of charge state and temperature for various base compositions. An exceptionally strong dependence of the decay rate on base composition has been identified. The physical basis for this process will be discussed. (J Am Soc Mass Spectrom 2003, 14, 1330–1339) © 2003 American Society for Mass Spectrometry

The structures and conformational changes of biomolecules in the gas phase have been studied by a variety of methods [1, 2]. One of the advantages of working in the gas phase is that it provides an opportunity to observe dynamical processes which may be obscured or not present in a condensed phase environment. Quadrupole ion traps provide a controlled environment in which ions can be probed for a theoretically unlimited time while in thermal equilibrium with the surrounding buffer gas. Ion trap instrumentation developed in our laboratory [3] has been used to carry out fluorescence measurements of trapped ions, and recently has been used to measure fluorescence resonance energy transfer (FRET) in trapped oligonucleotide ions [4]. The extension of FRET methods, widely used in solution studies [5], to measurements of trapped biomolecule ions provides the opportunity to *directly* correlate changes in fluorescence intensity with changes in the average conformation of biomolecules.

This paper describes the application of ion trapping technology and fluorescence measurements to the study of oligonucleotides in the gas phase. First, the unique capability of correlating in-situ fluorescence with mass spectra allows the investigation of the gas-phase dissociation dynamics of double-stranded oligonucleotide anions, and a continuation of previous studies [4] will be presented. The results of FRET and mass spectrometry experiments with trapped 14-mer double-stranded oligonucleotides display characteristics consistent with an intermediate state related to the dissociation dynamics into single strands. Second, the ability to store ions for long periods in controlled thermal environments has led to the observation of electron autodetachment of multiply charged oligonucleotide anions. The time and temperature dependence of the detachment rates and the dependence of these rates on the specific oligonucleotide sequence have been determined. It will be suggested that both processes are related to changes in the oligonucleotide conformation.

Experimental

Samples

Unmodified, desalted oligonucleotides were obtained commercially (Synthegen Modified Oligonucleotides, Houston, TX) and were used without further purification. Final solution concentrations for nanoelectrospray ionization (nESI) of the unmodified single-stranded oligonucleotides were 5 to 10 μM in 70/20/10 Metha-

Published online October 4, 2003

Address reprint requests to Dr. J. H. Parks, The Rowland Institute at Harvard, 100 Edwin H. Land Blvd., Cambridge, MA 02142, USA. E-mail: parks@rowland.harvard.edu.

1044-0305/03/$30.00
doi:10.1016/S1044-0305(03)00578-6

Received May 16, 2003
Revised July 28, 2003
Accepted July 30, 2003

nol/Water/Trifluoroethanol. Oligonucleotides derivatized with fluorophore molecules were obtained commercially (Synthegen) and were purified with reverse-phase HPLC prior to shipment. The fluorophore molecules are from the BODIPY line of dyes (Molecular Probes, Eugene, OR) and have N-succinimydil ester groups that react with amino functionalities present on either the 5′ or 3′ ends of the oligonucleotides. The donor fluorophore was BODIPY-Tetramethylrhodamine (BODIPY-TMR) and the acceptor fluorophore was BODIPY-Texas Red (BODIPY-TR). The sequences obtained were BODIPY-TR-5′-AAAAAAAGGCCGGC-3′ and 5′-GCCGGCCTTTTTTT-3′-BODIPY-TMR. Structures and absorption and emission data for the BODIPY fluorophores are available elsewhere [4, 6]. To form the oligonucleotide duplexes, the complementary single strands were combined at a concentration of 50 μM in a 50 mM ammonium acetate solution and annealed for 8 min at ~90°C, then slowly cooled to room temperature over 2–3 h. Because the single-stranded oligonucleotides have higher extinction coefficients than the double-stranded oligonucleotide, thermal denaturation of the duplexes with UV spectrophotometric detection was performed to confirm the presence of the duplexes in solution below the melting temperature of the duplex. Final concentrations for these nESI solutions of derivatized, annealed oligonucleotides were 5 to 10 μM in 50/50 methanol/water or 60/20/20 acetonitrile/isopropyl alcohol/water, with the final ammonium acetate concentration between 5 and 10 mM.

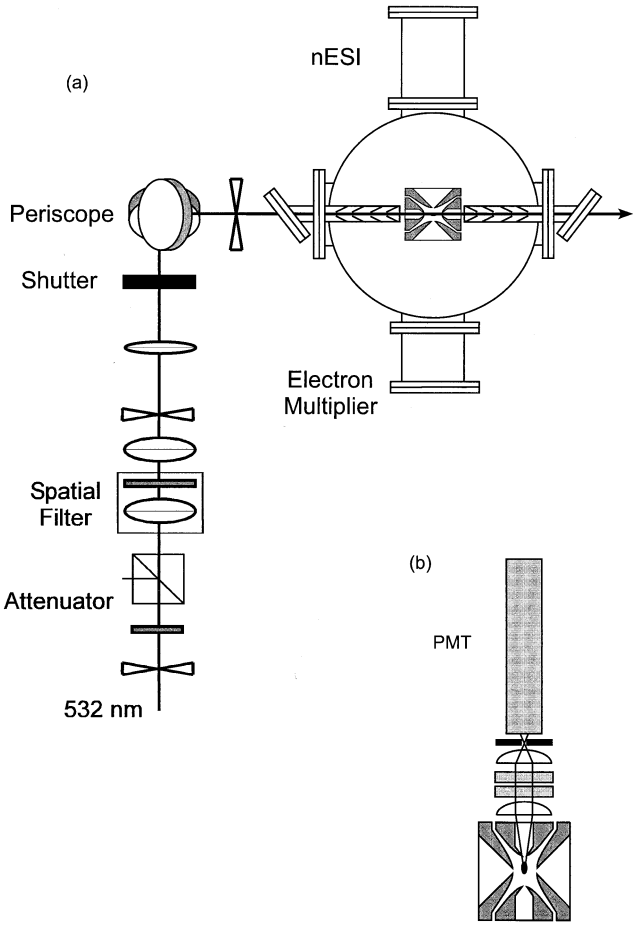

Figure 1. (**a**) Illumination optics used to direct the laser beam into the trapping volume; (**b**) 90° rotation of view of ion trap showing photomultiplier tube detection.

Ion Trap Mass Spectrometry

Experiments were conducted in a custom-built quadrupole ion trap described previously [3]. Ions are sprayed directly into a stainless steel capillary contained in a cylindrical copper block heated by cartridge heaters (Watlow, St. Louis, MO), and then travel through several ion optics and an octopole guide into the quadrupole ion trap. The trap electrodes and He gas inlet are seated in a copper housing which is resistively heated up to a maximum temperature of 170 °C (Model 965 temperature controller, Watlow) with a temperature precision of ±1 °C. The He bath gas pressure was ~0.4 mTorr and was pulsed to ~1 mTorr before loading ions into the ion trap. Isolated parent ions were held in the ion trap for a variable time period, and all ions were ejected at q_z = 0.908 and detected. A residual gas analyzer (Quadrex 200, Leybold, Export, PA) also is mounted on the vacuum system for detection of very low *m/z* species.

Fluorescence

Fluorescence analysis in the quadrupole ion trap has been described in detail [3]. The isolated ions of interest are irradiated with Nd:YAG laser pulses (~15 ns 100 Hz) at the frequency doubled wavelength 532 nm. The illumination optics used to direct the laser beam into the trapping volume are shown in Figure 1. The laser beam diameter has been reduced to ~150 μm to eliminate scattering on trap apertures and electrodes. The resulting laser-ion interaction is limited to a volume of $\sim 10^{-5}$ cm^3 which is ~0.03–0.15 of the total ion cloud volume, depending on trap operating parameters and temperature. An illustration of the volume of overlap between the laser beam and ion cloud is shown in Figure 2. The bandpass filter used for these experiments passes wavelengths 535 to 580 nm, corresponding to the donor fluorescence bandwidth [4, 6]. Thus, only the donor fluorescence was detected. The fluorescence was focused through an aperture of ≤1 mm positioned before a photomultiplier detector (PMT, Hamamatsu R1463). This limited the fluorescence collection to a solid angle defined by the laser-ion interaction volume which helped to minimize the detection of background laser scattering. Zero background detection has been achieved through this elimination of background laser scattering during the laser excitation pulse [3].

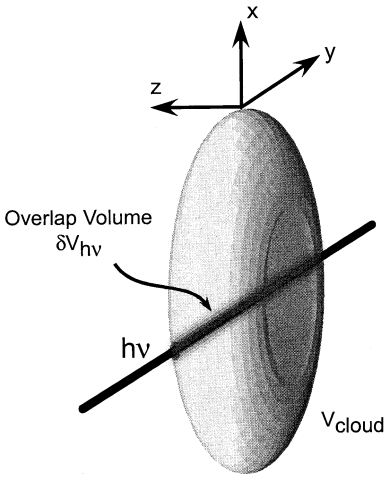

Figure 2. Illustration of the overlap volume ($\delta V_{h\nu}$) of the laser beam ($h\nu$) with the ion cloud (V_{cloud}) inside the quadrupole ion trap.

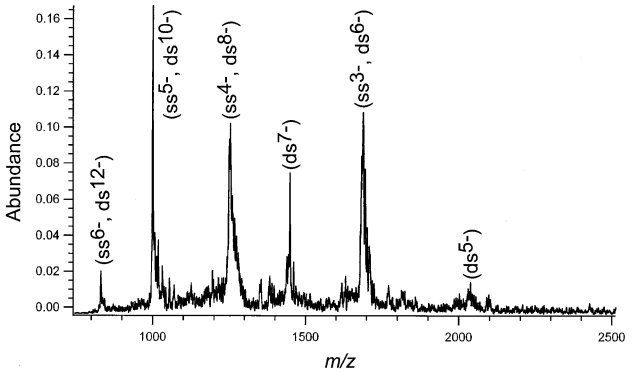

Figure 3. nESI-MS of the annealed solution of BODIPY-TR-5′-AAAAAAAGGCCGGC-3′ and 5′-GCCGGCCTTTTTTT-3′-BODIPY-TMR. Single strands are labeled "ss", double strands are labeled "ds".

Results and Discussion

FRET Measurements of Trapped Oligonucleotides

Changes in donor fluorescence from intact duplex ions have been observed recently with our instrumental setup [4]. The threshold of unzipping of the duplex of BODIPY-TMR-5′-AATTAATCCGGCCG-3′/5′-CGGC-CGGATTAATT-3′-BODIPY-TR was characterized by the detection of a small increase in donor fluorescence over the temperature range 109–123 °C. The temperature dependence of the fluorescence displayed qualitative agreement with a model calculation of the fraying dynamics [4]. Fluorescence measurements from the intact duplex ions at higher temperatures, where larger fluorescence intensities are expected because of the predicted increased distance between the ends of the double-stranded oligonucleotides containing the fluorophores, were not possible because of the amount of fragmentation of the duplex ions that occurred. Primarily, base loss from both strands of the duplex was observed. In an attempt to design a duplex that would undergo less fragmentation before undergoing separation into single strands, the sequence AAAAAAAGGC-CGGC and its complement was chosen. This choice was based on the mass spectra acquired with our instrument of AAAAAAA (A_7), TTTTTTT (T_7), and ATATATA, in which less fragmentation was observed in the spectra of A_7 and T_7 than ATATATA. Also, BIRD experiments conducted in an FTMS instrument showed that partially complementary duplexes of AATTAAT fragmented significantly more than complementary duplexes of A_7:T_7 [7].

A mass spectrum from the annealed solution of the BODIPY-TR-5′-AAAAAAAGGCCGGC-3′ (MW 4974) and 5′-GCCGGCCTTTTTTT-3′-BODIPY-TMR (MW 4954) is shown in Figure 3. Single strands of both 14-mers as well as even charge state ions of the 14-mer duplexes appear at similar *m/z* values which are not resolvable in this mass spectrum. The peaks labeled ds^{7-} and ds^{5-} are unambiguously identified as intact duplexes, so the 7- charge state of the 14-mer duplex was isolated for further analysis. After the ions of interest were isolated, they were held in the ion trap at a specific temperature and irradiated with the laser beam for 90 s. Figure 4 shows the mass spectrum acquired after 90 s irradiation, and the fluorescence spectrum acquired during the 90 s irradiation period. These spectra arise from a single loading of ions generated by nESI. The temperature in the trap was 133°C and the parent ion was held at a q_z of 0.54. The virtual absence of background laser scattering is demonstrated by comparing the fluorescence spectrum in Figure 4b to the PMT signal acquired when no ions were loaded into the trap, shown in Figure 4c. The fluorescence shown in Figure 4b is known to arise from the donor fluorophore which is attached to one of the two strands that makes up the noncovalently bound duplex because no other ions were present in the trap during the time of fluorescence data acquisition, as demonstrated in the mass spectrum shown in Figure 4a.

The experimental sequence illustrated in Figure 4 was repeated over a range of ion temperatures. Figure 5 shows the summed fluorescence intensities from each fluorescence spectrum as a function of temperature. The 7- duplex ions reached the fragmentation threshold for 90 s heating periods at 140 °C (dashed vertical line). The donor fluorescence does not change upon fragmentation, indicating that the separation between the fluorophores was large across the temperature range shown in Figure 5. The degree of fragmentation in the mass spectra above 140 °C is still relatively low (~4% at 166 °C), but fragment ion intensities can be increased for identification by using longer thermal exposure times. Such a spectrum is shown in Figure 6, where it can be seen that all fragment ions are due to cleavage of bonds between the A·T portion and G·C portion of the oligonucleotides, i.e., the formation of 7-mer strands.

The donor fluorescence intensities shown in Figure 5 are directly related to the distance between the donor

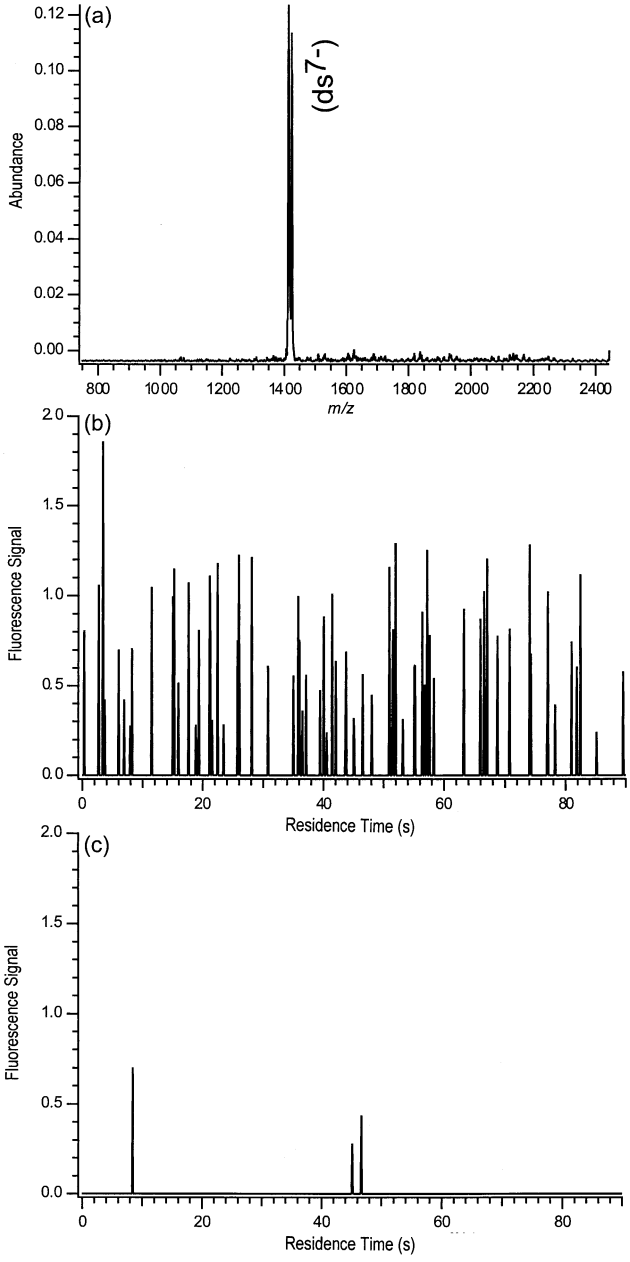

Figure 4. (**a**) Mass spectrum of the isolated 7- charge state of the duplex BODIPY-TR-5′-AAAAAAAGGCCGGC-3′ and 5′-GCCG-GCCTTTTTTT-3′-BODIPY-TMR after 90 s irradiation; (**b**) PMT signal over the 90 s irradiation period; (**c**) PMT signal over a 90 s irradiation period during which no ions were loaded into the ion trap.

and acceptor fluorophores conjugated to the strands of the duplex. The distance can be estimated by comparing the intensity of the donor fluorescence from the duplex to the intensity of the donor fluorescence from the singly-labeled strand. The fluorescence intensity at ~140 °C from the singly-labeled strand is shown in Figure 5, and this intensity is taken to be constant over the entire temperature range because it has been shown that the BODIPY quantum yields do not vary as a function of temperature [4]. The Förster distance, or the

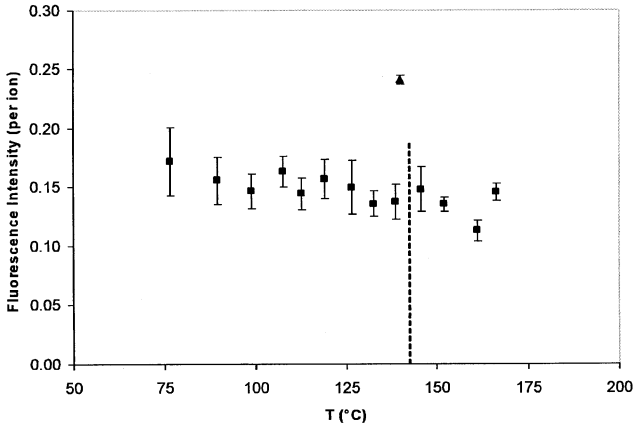

Figure 5. (filled square) Donor fluorescence intensity from the 7- charge state of the duplex BODIPY-TR-5′-AAAAAAAGGC-CGGC-3′ and 5′-GCCGGCCTTTTTTT-3′-BODIPY-TMR as a function of temperature. Error bars represent the standard deviation for triplicate measurements. At temperatures above the dashed line, fragment ions appeared in the mass spectrum acquired at the end of the 90 s irradiation periods. (filled triangle) Donor fluorescence intensity from the 6- charge state of 5′-GCCGGCCTTTTTTT-3′-BODIPY-TMR.

distance at which the FRET rate reduces the donor fluorescence by approximately a factor of 2, was taken to be 52 Å based on solution phase measurements [8]. The average separation between the fluorophores was calculated to be ~55 Å. If the duplex were to adopt a conformation in which only the G·C portion of the sequences were paired and the fluorophores were maximally separated, then the distance between fluorophores would be the sum of the lengths of the A·T portions of the oligonucleotides, ~48 Å, and the sum of the lengths of the C_6 amino linkers used to conjugate the dyes to the oligonucleotides, ~12 Å. The average separation of ~55 Å estimated from the data in Figure 5 is

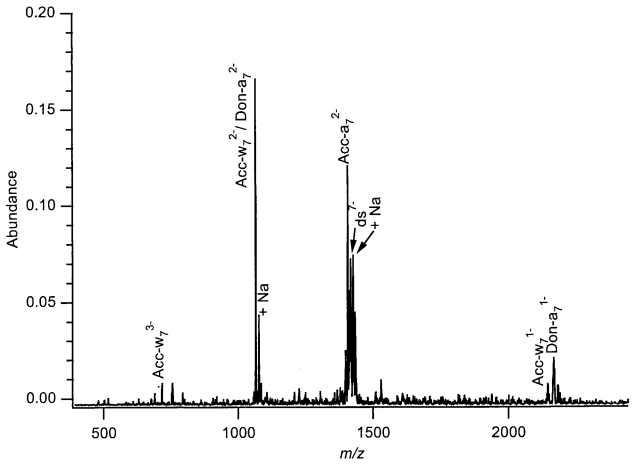

Figure 6. Thermal dissociation spectrum of the 7- charge state of the duplex BODIPY-TR-5′-AAAAAAAGGCCGGC-3′ and 5′-GC-CGGCCTTTTTTT-3′-BODIPY-TMR after 20 min heating at 160 °C. Fragment ions related to the strand labeled with BODIPY-TR labeled "Acc". Fragment ions related to the strand labeled with BODIPY-TMR labeled "Don".

consistent with the almost complete unpairing of the A·T section of the duplex. The estimated average distance, as well as the fragmentation of the duplex between the A·T and G·C segments, supports the conclusion that the separation between the fluorophores is large over the temperature range studied in the gas phase. The mass spectra acquired at the end of each irradiation period are crucial for the verification that the duplex ions were intact, and that the distance between the fluorophores arose from the fraying of the A·T ends of the duplex.

Electron Autodetachment of Single Strand Oligonucleotides

The conversion of a single isolated charge state, $M^{n}-$, of double-stranded oligonucleotides to the next lowest charge state, $M^{(n-1)-}$, was observed when ions were held in the ion trap under the heating and temporal conditions used in the FRET measurements. Subsequent measurements on fluorophore-derivatized single strands indicated that (1) the total ion count and fluorescence strength were approximately constant during the laser excitation interval, and that (2) laser excitation was not required for the charge state conversion to occur. This charge state conversion was characterized further in the absence of laser irradiation. It was observed that the oligonucleotides underwent sequential loss of charge with time, as shown in the mass spectra of Figure 7. The 4- charge state of 5′-T_7-3′-BODIPY-TMR was isolated in Figure 7a and held at 123 °C at $q_z = 0.50$ for Figure 7b 30 s and Figure 7c 960 s. A plot of the changes in the peak ion intensities from 0 to 960 s are shown in Figure 8. Rate equations were solved to describe the first order exponential decay/growth curves observed for the conversion of $M^{4-} \rightarrow M^{3-} \rightarrow M^{2-}$. The decay rates derived from single exponential data fits shown in Figure 8 are $k_{4\text{-}3} = 14.1\ (\pm 0.3) \times 10^{-3}\ s^{-1}$, $k_{3-2} = 0.60\ (\pm 0.05) \times 10^{-3}\ s^{-1}$, and the growth rate $k_2 = 0.59\ (\pm 0.03) \times 10^{-3}\ s^{-1}$.

This charge loss phenomenon also was found to occur for underivatized oligonucleotides. Figure 9 shows an example of the charge loss from $(A_7)^{3-}$. The isolation of $(A_7)^{3-}$ is shown in Figure 9a, and the resulting spectrum acquired after holding $(A_7)^{3-}$ in the ion trap for 240 s at 102 °C is shown in Figure 9b. No methods of activation other than thermal heating were used to produce the spectrum shown in Figure 9b. The two spectra in Figure 9 are plotted on the same absolute intensity scale, thus showing the ion population is conserved from Figure 9a to Figure 9b. The q_z of the isolated $(A_7)^{3-}$ ions was 0.38, resulting in a cutoff *m/z* of approximately 300 Da. Few of the typical product ions expected from dissociation (a- and w-type ions, ions resulting from base loss [9, 10]) of oligonucleotides in the ion trap would be predicted to appear below this cutoff *m/z*. Regardless, the possibility of additional fragment ions appearing outside the detected *m/z* range is negated because of the conservation of the total ion intensity between Figure 9a and b.

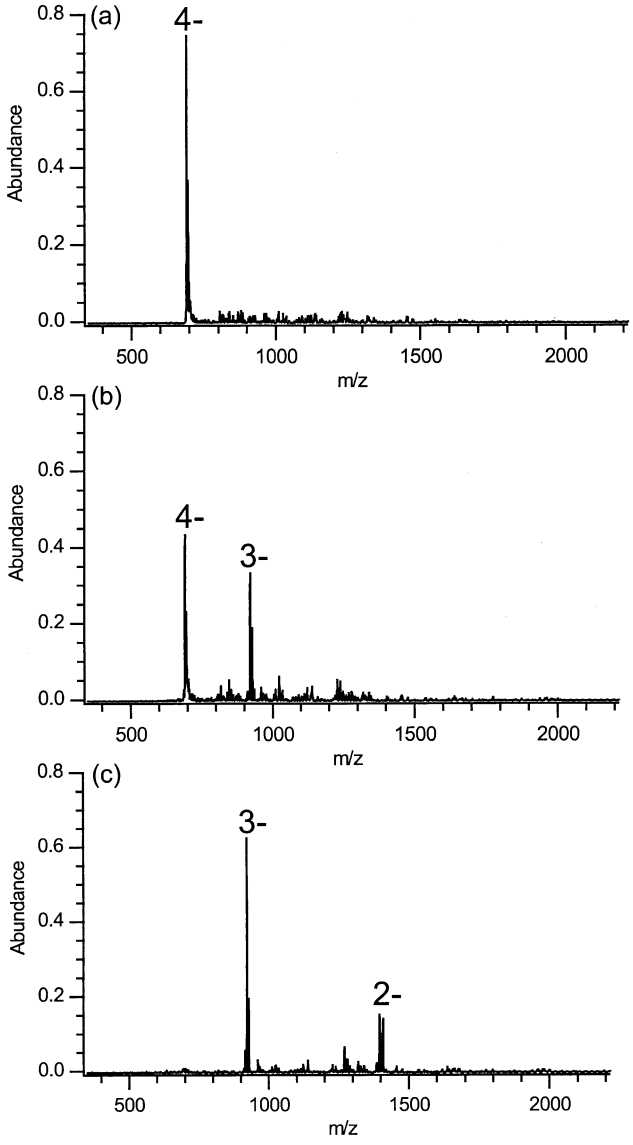

Figure 7. Mass spectra of 5′-T_7-3′-BODIPY-TMR at various heating times at 123°C. (**a**) 0 s (isolation of 4- charge state); (**b**) 30 s; (**c**) 960 s.

We attribute the observed charge loss to result from electron autodetachment. Several pieces of evidence support this conclusion: (1) The deconvoluted mass spectra display no evidence of change in molecular weight for the newly formed lower charge state ions. (2) No additional fragment ions appear in the mass spectrum that could be a result of an electron-abstraction or other ion-molecule reaction involving the higher charge state ion of the oligonucleotide. (3) Residual gas analyzer measurements showed no presence of hydrocarbons up to 200 amu in the vacuum system, and no significant changes in background gas pressures (CH_2/N, CO/N_2, O_2) at room and elevated temperatures. The only exception was a ~3× increase in water

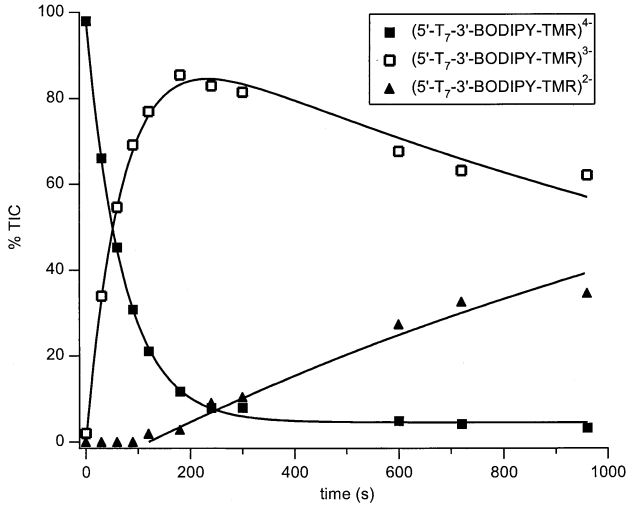

Figure 8. Change in ion intensities of 5′-T_7-3′-BODIPY-TMR as a function of heating time at 123 °C. Solid lines are curves fitted to data.

vapor content over the temperature range of 34 to 147 °C.

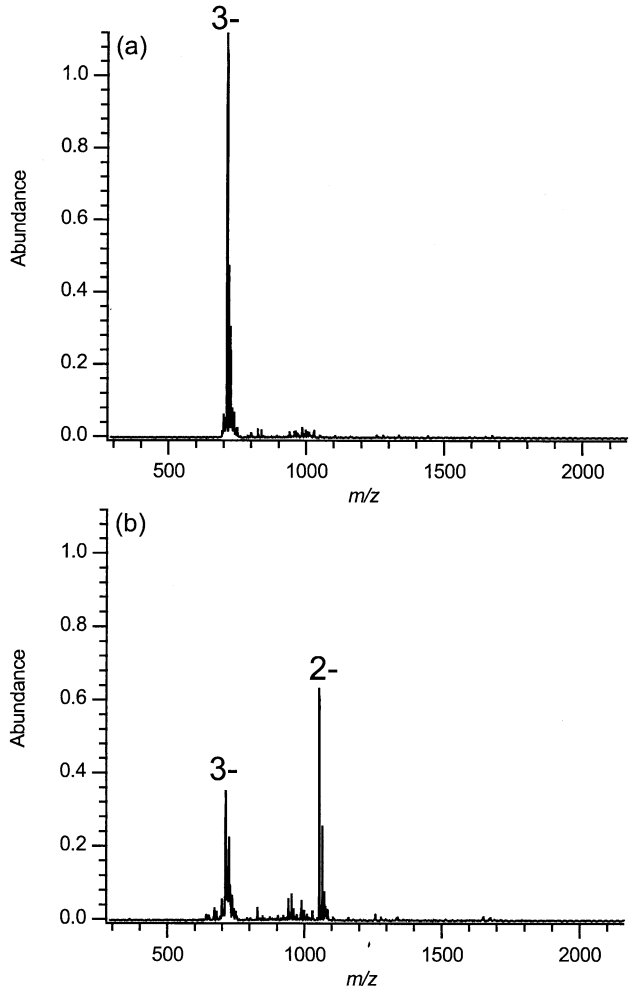

Figure 9. Mass spectra of A_7 at various heating times at 102 °C. (**a**) 0 s (isolation of 3- charge state); (**b**) 240 s.

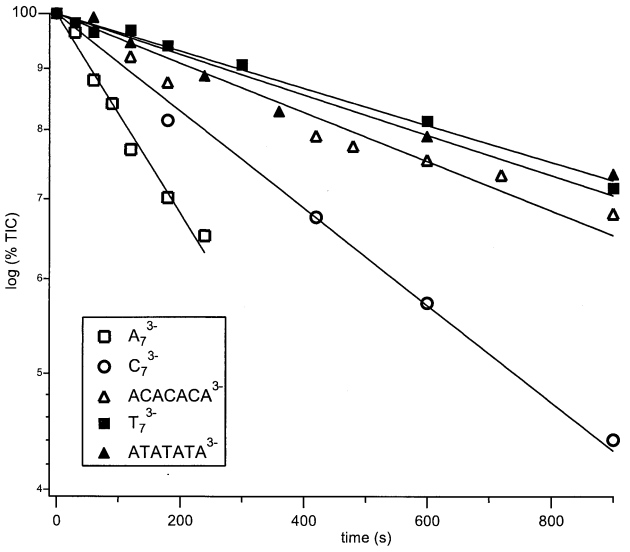

Figure 10. Change in ion intensities of 3- charge state of 7-mers as a function of heating time at 102 °C. Solid lines are curves fitted to data.

The rate at which electron autodetachment occurred for $(A_7)^{3-}$ was determined by varying the time the isolated 3- charge state ions were held at a given temperature and monitoring the intensities of the peaks in the mass spectrum. Similar experiments were conducted using $(T_7)^{3-}$, $(ATATATA)^{3-}$, $(ACACACA)^{3-}$, and $(C_7)^{3-}$ as the analytes. Figure 10 shows the decrease in the percent total ion current (plotted as log %TIC) for these 7-mers as a function of the time the ions were held in the ion trap at 102 °C at $q_z = 0.38$. Arrhenius plots of the electron autodetachment rates for the five 7-mers analyzed are shown in Figure 11 over the temperature range studied, ~102 to 150 °C. As shown in Figure 8, the electron autodetachment rate constants were determined from exponential fits of the data. Uncertainties in the $\ln(k_{32})$ values in Figure 11 arising from these data fits were a few percent (not shown). Across this tem-

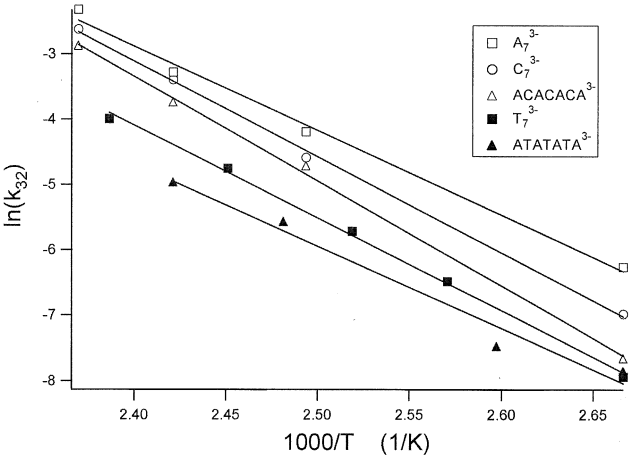

Figure 11. Arrhenius plots of the electron autodetachment rates for the 3- charge state of 7-mers with different base compositions. Solid lines are linear fits to the data.

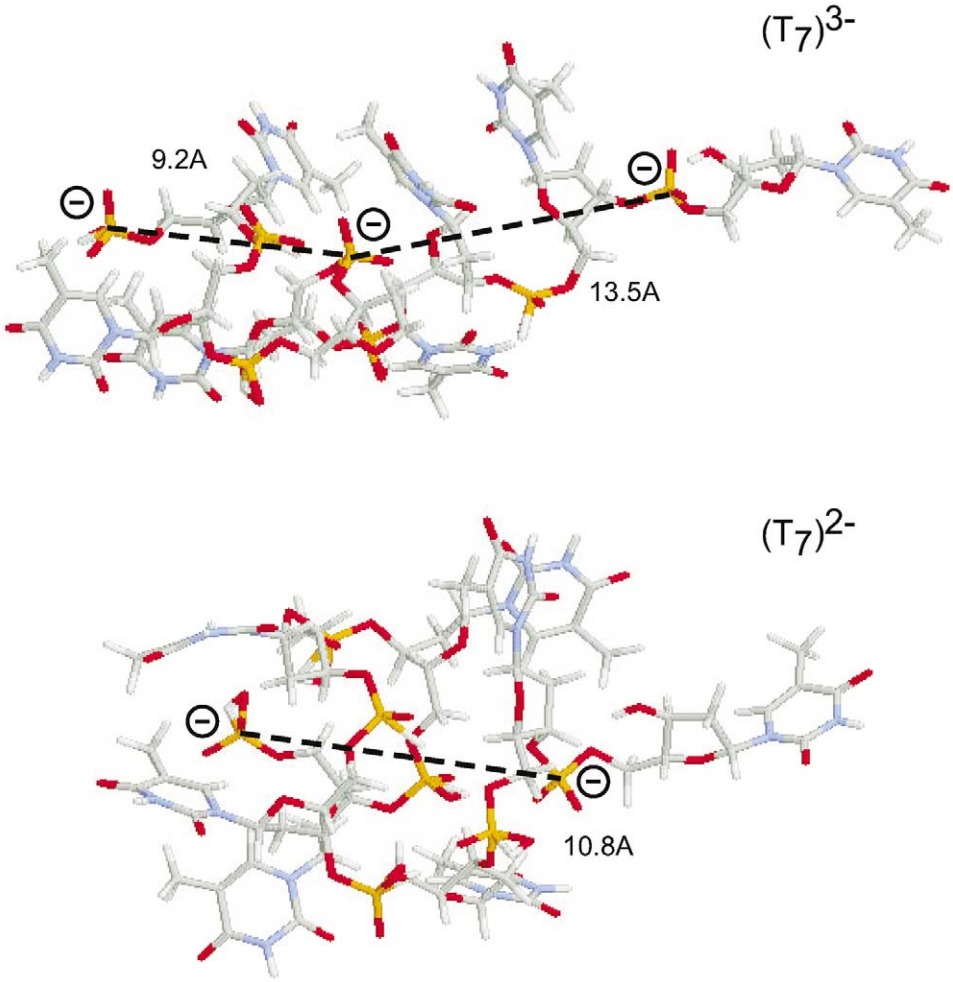

Figure 12. Structures of the 3- and 2- charge states of T_7 calculated by molecular dynamic simulations. The dashed lines are drawn between negatively charged phosphates and the spatial separations are indicated.

perature range, the electron autodetachment rates vary as a function of the oligonucleotide sequence. The implications of this trend of will be discussed below.

Experimental measurements of electron autodetachment processes have been carried out for small organic molecules [11–14] and atomic clusters [15, 16]. In these measurements, electron detachment occurred after vibrational heating via multiphoton infrared absorption. Theoretical calculations of the non-adiabatic processes associated with electronic curve-crossings [17–19] have been applied to describe the transfer of vibration to electronic energy in these smaller molecules. Photoelectron spectroscopy studies of small, more rigid molecules have measured [20] the electron detachment energies which characterize multiply charged anion electronic states. One of the more interesting results derived from the photodetachment measurements [21] of benzene dicarboxylate dianions is the variation of detachment energies for three different structural isomers for which the electron charge separations are different.

The electron autodetachment from single strand oligonucleotides presumably involves a similar vibration to electronic transfer processes. However, in contrast to the smaller molecules whose structure is compact and fairly rigid, the oligonucleotide structure for a single strand can be quite flexible and can vary depending on charge state, temperature and base composition. For example, it is illustrative to examine structures as a function of charge state. Molecular dynamics simulations of $(T_7)^{3-}$ and $(T_7)^{2-}$ structures at 298 K were performed [22] using InsightII software. Structures were initially relaxed with a gradient method and the simulation was performed for 3 ns using an extensible systematic forcefield (esff) having parameters optimized for a vacuum environment. Negative charges were localized on the phosphate groups at the center and ends of the $(T_7)^{3-}$ structure and on the ends of the $(T_7)^{2-}$ structure. Figure 12 shows preliminary results for these structures which display considerable distortion of the single strand conformation. The $(T_7)^{3-}$ conformation is more extended with a distance between end charges of ~22.2 Å whereas the end charges on $(T_7)^{2-}$ are separated by ~10.8 Å.

The calculated conformations shown in Figure 12 are not intended to represent global minimum energy structures, but merely to indicate that the increased single strand flexibility can lead to large changes in the charge separations. One of the more informative pieces of data that will be derived from continuing MD simulations are histogram analyses of anion separations over the simulation time. Although the electron affinity of the phosphate group is approximately 5 eV, from measurements [23] and calculations [24] of the dihydrogen phosphate anion, in the presence of reduced charge separations the detachment energy can be significantly lowered as a result of increased Coulomb repulsive forces. This suggests that the electron autodetachment of a multiply charged oligonucleotide anion can be correlated with the biomolecular conformation by comparing autodetachment data with the predicted structures derived from molecular dynamic simulations. Two types of calculations are underway to investigate the autodetachment process in oligonucleotides: (1) Molecular dynamic simulations [25] to determine the distribution of charge separations for the single stranded oligonucleotides at relevant temperatures, and (2) applying the simulation results to estimate the Coulomb interactions and the charge-induced perturbations of the phosphate electronic states leading to detachment [26] including the screening effects related to the dipole moment of the bases.

It is relevant to consider how correlations between oligonucleotide conformation and autodetachment data can qualitatively describe the dependence of the decay rates on charge state, temperature and base composition.

Charge state. The flexibility of single strands may depend in part on the charge state of the anions [27]. Fluctuations which reduce the distance between charges will have a greater probability of lowering the detachment energy barrier because the coulomb repulsion at any specific charge state decreases with decreasing charge state. The possibility for repulsive Coulomb barriers to be determined by structural fluctuations is the principle difference between electron detachment from oligonucleotides and from smaller, rigid molecules. In the presence of such fluctuations, the transition between the n- and $(n-1)$-oligonucleotide charge states may be more correctly described as a transition between the electronic state of a singly charged phosphate anion and the neutral state driven by fluctuating Coulomb fields.

The discussion here refers to the ensemble average of the charge separations since each oligonucleotide of a given charge state will in principle have charges positioned on a different set of phosphate sites. It is an interesting question whether the anions in the nESI solution phase have an ensemble charge distribution which peaks at separations which minimize the Coulomb energy, or if charge solvation reduces the advantage gained by forming such a minimum energy state.

Temperature. The increase of autodetachment rates with temperature shows an interesting behavior: different charge states and different base compositions display Arrhenius plots having similar slopes as shown in Figure 11. The linear fits of these data yield enthalpy barriers for electron loss of $\Delta H \sim 0.95$ to 1.05 eV. The more significant variation in the temperature dependence of the rates appears to be determined by the entropic contribution related to the intercepts in Figure 11. The Arrhenius prefactors for different sequences derived from the intercepts are 1.2×10^{11} s^{-1} for ATATATA; 1.6×10^{12} s^{-1} for A_7; 9.7×10^{12} s^{-1} for T_7; 8.7×10^{13} s^{-1} for C_7; 1.8×10^{15} s^{-1} for ACACACA.

It is not clear at this point just what the apparent enthalpy barrier represents. The increase in temperature can influence the autodetachment rate in several ways. The overall flexibility of the oligonucleotide will increase as higher vibrational modes are populated and this can increase the probability of charge proximity. The excitation of higher vibrational states of the phosphate anion would increase the rate of electron loss providing the non-adiabatic curve crossing associated with the detachment transition occurs at higher vibrational levels. In any case, the observed similarity of the enthalpy barriers could be derived from the phosphate vibronic state dynamics which will be common to the detachment process independent of charge state and base composition. Assuming the similarity of the slopes for different base sequences is related to the phosphate moiety of the nucleotide, it is interesting that the rates derived from the prefactors show much greater variation. This suggests that the phase space pathways to the transition state for electron loss may rely on the molecular dynamics of a greater portion of the oligonucleotide than simply the phosphate.

Another contribution to the energy required to excite the vibrational modes associated with detachment may be supplied by fluctuations of the internal energy at the RRKM rate. Note that at a temperature of 300 K, equipartition of the vibrational modes of 7 thymine nucleotides will have a total internal energy of ~17 eV. Although measurements of the decay rates of fluorophore-derivatized oligonucleotides have not been central to these analyses of simpler structures, these species displayed increased detachment rates in the presence of laser excitation which depended on the laser intensity. A statistical distribution of vibrational energy resulting from a single photon of energy 2.33 eV corresponds to a temperature increase of $\Delta T \sim 42$ K which would lead to a significant increase in the detachment rates shown in Figure 11. An estimate of the RRKM rates will be obtained from the vibrational frequencies calculated by the molecular dynamic simulations to determine if statistical fluctuations can yield a significant contribution on the timescale of the detachment rate.

Base composition. One of the most interesting results of these measurements is the strong dependence of the autodetachment rates on the base composition of the

oligonucleotides. The data displayed in Figure 10 indicate the electron autodetachment rates of $(T_7)^{3-}$ and $(A_7)^{3-}$ differ by a factor >5. There are several properties which depend on base composition under consideration which might be associated with this variation. Although the hydrogen bonding energetics associated with Watson-Crick pairing have been shown [7, 28] to be consistent with gas phase measurements of the thermal dissociation of oligonucleotide duplexes, the presence of base stacking interactions has not been identified previously in gas phase studies. The flexibility of single strands have been correlated with base stacking interactions in recent solution phase studies of the dynamics of single strand oligonucleotides [29–31]. The strong dependence of these interactions on base composition and sequence suggest a possible mechanism for the observed sequence dependence of electron autodetachment rates. For example, the solution phase experiments indicate that the base stacking energy of poly(A) is greater than that of poly(T) which could lead to smaller average spatial fluctuations of A_7. However, the greater flexibility expected for T_7 would enable the formation of more compact conformations which could shield the Coulomb fields more effectively.

Dielectric screening of the Coulomb fields in a gas phase environment will be introduced by the dipole moments of the bases and the polarizability of the nucleotides. These screening contributions will be sensitive to both the composition and sequence of the oligonucleotide. Molecular dynamics simulations will provide an insight how to configure base compositions and sequences to vary the both the base stacking and the screening interactions independently to identify their contributions to the autodetachment rate.

Conclusions

These experiments demonstrate that measurements of the fluorescence of trapped biopolymer ions can be achieved with sufficient sensitivity and dynamic range to observe FRET signatures associated with the conformations of gas phase ions. These studies help to evaluate possibilities for extending such measurements to other dynamical processes. Many systems are available for the application of FRET techniques presented here to study conformational changes characteristic of folding transitions in the gas phase, such as the opening and closing transitions of DNA hairpins [32, 33]. In the planned research, fluorophore excitation will be performed with a continuous wave laser at 532 nm. A two-channel detection system will be used to simultaneous monitor donor and acceptor fluorescence, essential for verification and interpretation of results.

The electron autodetachment process observed here in gas phase studies would probably not be observable in a condensed phase environment since solvation of the phosphate anion sites would strongly screen the Coulomb fields. In gas phase, autodetachment appears to be a process which involves the confluence of several physical interactions which probably accounts for the slow detachment rates. Analysis of the detachment data will require calculations at different molecular levels to evaluate the principle conclusions:

- Electron autodetachment in multiply-charged anion environment is assumed to be primarily driven by conformational fluctuations which determines the rate dependence on charge state;
- temperature dependence of these rates can result from the population of vibrational levels involved in the nonadiabatic curve crossing of phosphate anion electronic states, perhaps with contributions from RRKM fluctuations;
- strong dependence of detachment rates on base composition and sequence can be related to both stacking interactions between bases within the anion environment, and also dielectric screening effects of the nucleotides.

Measurements of electron autodetachment provide a unique opportunity to investigate oligonucleotide dynamics in the gas phase. It remains an open question how best to take advantage of this new probe. Continuing research will consider in more detail the degree to which the detachment depends on base composition by configuring sequences to distinguish between the properties of flexibility and dielectric screening. In addition, FRET experiments of dual-labeled oligonucleotides are currently underway to determine if a correlation exists between the flexibility of the oligonucleotide anion and its charge state.

Gas phase measurements are an important initial step in performing experiments on biomolecules as a function of hydration. Much can be learned if these experiments can be performed as a function of the level of hydration. Such measurements can address the effect of water interactions with hydrogen bonds, charge sites and processes leading to local entropy variations. A goal of this research is to extend the methods discussed in this paper to experiments performed as a function of hydration level.

Acknowledgments

This work has been funded by The Rowland Institute at Harvard. JHP acknowledges Holger Merlitz and Wolfgang Wenzel for discussions and preliminary molecular dynamics simulations. He also thanks Tom Cheatham and Jack Simons for continuing discussions which have helped formulate an approach to calculations of the electron autodetachment process.

References

1. Hoaglund-Hyzer, C. S.; Counterman, A. E.; Clemmer, D. E. Anhydrous Protein Ions. *Chem. Rev.* **1999,** *99,* 3037–3080.
2. Jarrold, M. F. Peptides and Proteins in the Vapor Phase. *Annu. Rev. Phys. Chem.* **2000,** *51,* 179–207.

3. Khoury, J. T.; Rodriguez-Cruz, S. E.; Parks, J. H. Pulsed Fluorescence Measurements of Trapped Molecular Ions with Zero Background Detection. *J. Am. Soc. Mass Spectrom.* **2002,** *13,* 696–708.
4. DanellA. S.ParksJ. H. FRET Measurements of Trapped Oligonucleotide Duplexes. *Int. J. Mass Spectrom*2003in press.
5. Selvin, P. R. The Renaissance of Fluorescence Resonance Energy Transfer. *Nature Struct. Biol.* **2000,** *7,* 730–734.
6. Molecular Probes website, www.molecularprobes.com accessed May, 2003.
7. Schnier, P. D.; Klassen, J. S.; Strittmatter, E. F.; Williams, E. R. Activation Energies for Dissociation of Double Strand Oligonucleotide Anions: Evidence for Watson-Crick Base Pairing in Vacuo. *J. Am. Chem. Soc.* **1998,** *120,* 9605–9613.
8. Parkhurst, K. M.; Parkhurst, L. J. Donor-Acceptor Distance Distributions in a Double-Labeled Fluorescent Oligonucleotide Both as a Single Strand and in Duplexes. *Biochemistry* **1995,** *34,* 293–300.
9. McLuckey, S. A.; Vaidyanathan, G.; Habibi-Goudarzi, S. Charged versus Neutral Nucleobase Loss from Multiply Charged Oligonucleotide Anions. *J. Mass Spectrom.* **1995,** *30,* 1222–1229.
10. McLuckey, S. A.; Vaidyanathan, G. Charge State Effects in the Decompositions of Single-Nucleobase Oligonucleotide Polyanions. *Int. J. Mass Spectrom. Ion Processes* **1997,** *162,* 1–16.
11. Foster, R. F.; Tumas, W.; Brauman, J. I. Unimolecular Decomposition and Vibrationally Induced Electron Autodetachment of Acetone Enolate Ion. *J. Chem. Phys.* **1983,** *79,* 4644–4646.
12. Meyer, F. K.; Jasinski, J. M.; Rosenfeld, R. N.; Brauman, J. I. Infrared Multiphoton Photodetachment of Negative Ions in the Gas Phase. *J. Am. Chem. Soc.* **1982,** *104,* 663–667.
13. Woodin, R. L.; Foster, M. S.; Beauchamp, J. L. Ion Cyclotron Resonance Studies of Radiative and Dissociative Electron Attachment Processes at Low Pressures. *J. Chem. Phys.* **1980,** *72,* 4223–4227.
14. Wight, C. A.; Beauchamp, J. L. Infrared Spectra of Gas-Phase Ions and Their Use in Elucidating Reaction Mechanisms. Identification of $C_7H_7^-$ Structural Isomers by Multiphoton Electron Detachment Using a Low-Power Infrared Laser. *J. Am. Chem. Soc.* **1981,** *103,* 6499–6501.
15. Amrein, A.; Simpson, R.; Hackett, P. Multiphoton Excitation, Ionization, and Dissociation Decay Dynamics of Small Clusters of Niobium, Tantalum, and Tungsten: Time-Resolved Thermionic Emission. *J. Chem. Phys.* **1991,** *95,* 1781–1800.
16. Amrein, A.; Simpson, R.; Hackett, P. Delayed Ionization Following Photoexcitation of Small Clusters of Refractory Elements: Nanofilaments. *J. Chem. Phys.* **1991,** *94,* 4663–4664.
17. Clary, D. C. Vibrationally Induced Photodetachment of Electrons from Negative Molecular Ions. *Phys. Rev. A* **1989,** *40,* 4392–4399.
18. Acharya, P. K.; Kendall, R. A.; Simons, J. Vibration-Induced Electron Detachment in Molecular Anions. *J. Am. Chem. Soc.* **1984,** *106,* 3402–3407.
19. Simons, J. Propensity Rules for Vibration-Induced Electron Detachment of Anions. *J. Am. Chem. Soc.* **1981,** *103,* 3971–3976.
20. Wang, L.-S.; Wang, X.-B. Probing Free Multiply Charged Anions Using Photodetachment Photoelectron Spectroscopy. *J. Phys. Chem. A* **2000,** *104,* 1978–1990.
21. Wang, X.-B.; Nicholas, J. B.; Wang, L.-S. Intramolecular Coulomb Repulsion and Anisotropies of the Repulsive Coulomb Barrier in Multiply Charged Anions. *J. Chem. Phys.* **2000,** *113,* 653–661.
22. Wenzel, W.; Merlitz, H. Personal Communication, 2003.
23. Wang, X.-B.; Vorpagel, E. R.; Yang, X.; Wang, L.-S. Experimental and Theoretical Investigations of the Stability, Energetics, and Structures of $H_2PO_4^-$, $H_2P_2O_7^{2-}$, and $H_3P_3O_{10}^{2-}$ in the Gas Phase. *J. Phys. Chem. A* **2001,** *105,* 10468–10474.
24. Kuo, I.-F.; Tobias, D. J. Electronic Polarization and Hydration of the Dimethyl phosphate Anion: An ab Initio Molecular Dynamics Study. *J. Phys. Chem. B* **2001,** *105,* 5827–5832.
25. Cheatham, T. E. III. Personal Communication, 2003.
26. Simons, J. Personal Communication, 2003.
27. Okonogi, T. M.; Alley, S. C.; Harwood, E. A.; Hopkins, P. B.; Robinson, B. H. Phosphate Backbone Neutralization Increases Duplex DNA Flexibility: A Model for Protein Binding. *Proc. Natl. Acad. Sci. U.S.A.* **2002,** *99,* 4156–4160.
28. Gabelica, V.; De Pauw, E. Collision-Induced Dissociation of 16-mer DNA Duplexes with Various Sequences: Evidence for Conservation of the Double Helix Conformation in the Gas Phase. *Int. J. Mass Spectrom.* **2002,** *219,* 151–159.
29. Goddard, N. L.; Bonnet, G.; Krichevsky, O.; Libchaber, A. Sequence Dependent Rigidity of Single Stranded DNA. *Phys. Rev. Lett.* **2000,** *85,* 2400–2403.
30. Aalberts, D. P.; Parman, J. M.; Goddard, N. L. Single-Strand Stacking Free Energy from DNA Beacon Kinetics. *Biophys. J.* **2003,** *84,* 3212–3217.
31. Mills, J. B.; Vacano, E.; Hagerman, P. J. Flexibility of Single-stranded DNA: Use of Gapped Duplex Helices to Determine the Persistence Lengths of Poly(dT) and Poly(dA). *J. Mol. Biol.* **1999,** *285,* 245–257.
32. Wallace, M. I.; Ying, L.; Balasubramanian, S.; Klenerman, D. FRET Fluctuation Spectroscopy: Exploring the Conformational Dynamics of a DNA Hairpin Loop. *J. Phys. Chem. B* **2000,** *104,* 11551–11555.
33. Bonnet, G.; Krichevsky, O.; Libchaber, A. Kinetics of Conformational Fuctuations in DNA Hairpin Loops. *Proc. Natl. Acad. Sci. U.S.A.* **1998,** *95,* 8602–8606.